Since January 2020 Elsevier has created a COVID-19 resource centre with free information in English and Mandarin on the novel coronavirus COVID-19. The COVID-19 resource centre is hosted on Elsevier Connect, the company's public news and information website.

Biosensors and Bioelectronics 119 (2018) 79–85

Contents lists available at ScienceDirect

Biosensors and Bioelectronics

journal homepage: www.elsevier.com/locate/bios

Arch-shaped multiple-target sensing for rapid diagnosis and identification of emerging infectious pathogens

Bonhan Koo[a], Ki Ho Hong[b], Choong Eun Jin[a], Ji Yeun Kim[c], Sung-Han Kim[c,*], Yong Shin[a,*]

[a] Department of Convergence Medicine, Asan Medical Center, University of Ulsan College of Medicine, Biomedical Engineering Research Center, Asan Institute of Life Sciences, Asan Medical Center, 88 Olympicro-43gil, Songpa-gu, Seoul, Republic of Korea
[b] Department of Laboratory Medicine, Seoul Medical Center, Seoul, Republic of Korea
[c] Department of Infectious Diseases, Asan Medical Center, University of Ulsan College of Medicine, Seoul, Republic of Korea

ARTICLE INFO

Keywords:
Emerging infectious pathogen
Middle East respiratory syndrome
Zika
Ebola
Diagnosis
Pathogens identification

ABSTRACT

Rapid identification of emerging infectious pathogens is crucial for preventing public health threats. Various pathogen detection techniques have been introduced; however, most techniques are time-consuming and lack multiple-target detection specificity. Although multiple-target detection techniques can distinguish emerging infectious pathogens from related pathogens, direct amplification methods have not been widely examined. Here, we present a novel arch-shaped multiple-target sensor capable of rapid pathogen identification using direct amplification in clinical samples. In this study, an arch-shaped amplification containing primer sequences was designed to rapidly amplify multiple targets. Further, the sensing platform allowed for sensitive and specific detection of human coronavirus, Middle East respiratory syndrome, Zika virus, and Ebola virus down to several copies. This platform also simultaneously distinguished between Middle East respiratory syndrome and human coronavirus in clinical specimens within 20 min. This arch-shaped multiple-target sensing assay can provide rapid, sensitive, and accurate diagnoses of emerging infectious diseases in clinical applications.

1. Introduction

An increasing number of pathogens that cause unexpected illnesses and epidemics among humans and animals has led to the loss of life and economic problems (Sands et al., 2016; Allegranzi et al., 2011). Recently, emerging infectious diseases, such as Middle East respiratory syndrome-coronavirus (MERS-CoV) (Zaki et al., 2012), Ebola virus (EBOV) (Biava et al., 2018), and Zika virus (ZIKV) (Munoz-Jordan, 2017) outbreaks, have revealed that disease control systems require more effective and coordinated responses, including vaccine development, diagnostic tools, and therapeutics (Sands et al., 2016). According to the World Health Organization (WHO), an outbreak of MERS-CoV resulted in 1782 infections and 634 deaths in June 2016 (WHO, 2016). In 2015, MERS-CoV infiltrated South Korea, resulting in 186 infections and 39 deaths with high mortality rates of over 30% (WHO, 2015a; Rao and Nyquist, 2014). For more effective prevention of emerging infectious disease threats, rapid diagnostics are needed to identify new pathogens for which vaccines and effective therapeutics are not available.

Rapid diagnostics to identify and diagnose pathogens have been performed using nucleic acid-based detection techniques, such as end-point polymerase chain reaction (PCR) and real-time RT-PCR, as gold standard methods (Zumla et al., 2015; WHO, 2015b; CDC, 2016). While these methods are relatively sensitive and specific for pathogen detection, they have several limitations, including the long time to acquire results, high technicality, and costly equipment such as a thermal cycler (Yang and Rothman, 2004; Barken et al., 2007; Mori and Notomi, 2009; Huang et al., 2006). Additionally, multiplex detection techniques, which detect two or more targets simultaneously in a single reaction, are required to distinguish the target pathogen from similar family members and offers reduced time and reagent costs (Brinkmann et al., 2017; Chung et al., 2013). Multiplex detection techniques are critical for rapid diagnostics; however, self-inhibition and false-positive results caused by primer dimerization (from a primer-target template mismatch or primer itself) can reduce detection sensitivity and specificity in clinical applications. To overcome the limitations of multiplex detection, a solid-phase DNA amplification technique was developed by grafting both forward and reverse primers. However, the amplification efficiency of the grafting primer assay was approximately 90% lower than that of conventional PCR in solution (Adessi et al., 2000; Fedurco et al., 2006; Shendure and Ji, 2008). Thus, the solid-phase DNA amplification technique has not been widely explored for applications in

* Corresponding authors.
E-mail addresses: kimsunghanmd@hotmail.com (S.-H. Kim), shinyongno1@gmail.com (Y. Shin).

https://doi.org/10.1016/j.bios.2018.08.007
Received 21 May 2018; Received in revised form 24 July 2018; Accepted 7 August 2018
Available online 08 August 2018
0956-5663/

pathogen diagnostics. These limitations have made it difficult to apply diagnostic methods in hospitals. Resolving these limitations will require the development of diagnostic methods that are easy-to-use, accurate, and rapid for use in hospitals.

Here, we report a novel arch-shaped multiple-target sensing platform for rapid diagnosis and identification of emerging infectious pathogens. An isothermal amplification enzyme and oligonucleotide primers were immobilized on a silicon microring resonator (SMR) for specific detection of target nucleic acids from emerging infectious pathogens, such as MERS-CoV, Zika, and Ebola. In this study, rather than applying the amplified target and probe hybridization assay, we established long (> 50 base pair, bp) oligonucleotide primers at a high concentration (5 μM) to create an arch shape on the sensor surface for solid-phase amplification, thus overcoming primer dimerization. The SMR sensor allows for sensitive, label-free, and real-time sensing (Kim et al., 2018; Koo et al., 2017), and the long primers at a high concentration greatly increased the rate and detection sensitivity of this method. For nucleic acid amplification, we used a recombinase polymerase amplification (RPA) enzyme, which requires a small instrument for isothermal amplification (Piepenburg et al., 2006). Using the arch-shaped sensing platform, we detected RNA from human coronavirus (HCoV), MERS-CoV, ZIKA, and EBOV with high sensitivity and specificity. The detection limit was 10-fold more sensitive than that of real-time reverse transcription-PCR. Furthermore, this multiple-target sensing platform rapidly (< 20 min) detected MERS-CoV in 20 clinical specimens, including MERS-CoV and HCoV infections. Therefore, the arch-shaped multiple-target sensing platform can be used to rapidly identify pathogens in various clinical applications.

2. Material and methods

2.1. Development and operation of the arch-shaped multiple-target sensor

To use the arch-shaped multiple-target sensing platform as a multiple detection system, we structured the SMR sensor as previously described (Kim et al., 2018; Koo et al., 2017). For arch-shaped amplification and detection with specific primers immobilized on the sensor, a three-step primer modification was required on the surface of the sensing chip. First, amine group modification using 3-aminopropyltriethoxysiane (APTES, Sigma-Aldrich, St. Louis, MO, USA) was performed on the sensing surface. Subsequently, the sensors were treated with oxygenated plasma and soaked in a solution of 2% APTES in a mixture of ethanol–H_2O (95:5, v/v) for 2 h, followed by thorough rinsing with ethanol and deionized (DI) water. Second, carboxyl group modification was conducted using glutaraldehyde (GAD, Sigma-Aldrich) as a linker. The sensors were cured by heating to 120 °C for 15 min. Next, the sensors were incubated with 2.5% GAD in DI water containing 5 mM sodium cyanoborohydride (Sigma-Aldrich) for 1 h, rinsed with DI water, and dried under a nitrogen stream. Third, both forward and reverse primers were immobilized to target specific primers containing the 5′ amino-modifier C12. The pretreated sensor was prepared by overnight incubation at room temperature in a 5 or 10 μM solution of forward and reverse primers containing 5 mM sodium cyanoborohydride. After incubation, unbound target specific primers were removed by washing with phosphate-buffed saline and the sensors were dried using nitrogen. The prepared sensor chip was stored at room temperature until further use. To test the target amplification and detection in the primer immobilized sensor chip, recombinase polymerase amplification-reverse transcription (RPA-RT, TwistDx, Cambridge, UK) containing 29.5 μL of rehydration buffer, 15 μL of RNase inhibitor and water, 2 μM of DTT, recombinase, polymerase enzyme, and 2.5 μL of magnesium acetate solution. To start the reaction, 10 μL of RPA-RT solution and 5 μL of target RNA were mixed. Next, 15 μL of this mixture was added to the sensor chip with an acrylic well surrounding the microring sensor area. Additionally, mineral oil was added to prevent evaporation of the mixture during amplification. The arch-shaped multiple-target sensor assay was operated at a constant temperature (43 °C). The sensor consists of four rings connected to a common input and separate dedicated output waveguides. One of the four microrings was used as a reference sensor to monitor temperature-induced drift. The 3 remaining microrings were used for sensing three targets (MERS, EBOV, ZIKV) with a vertical grating coupler. For multiple target monitoring, each dedicated output waveguide corresponding to the microring immobilized different target specific primer was measured sequentially by moving the optical fiber. The tunable laser emits light at wavelengths of 1550–1580 nm (EXFO IQS- 2600B, Quebec, Canada). To obtain a baseline as a reference, the resonance wavelength was immediately measured. The resonance wavelength shift for multiple target detection was then measured every 5 min for up to 30 min to monitor the arch-shaped amplification of MERS, ZIKV, EBOV, and HCoV RNAs in a label-free and real-time manner.

2.2. Primer length and concentration for arch-shaped multiple-target sensing

We designed the Arch-RT-PCR primer based on genome sequence information for MERS, ZIKV, EBOV, and HCoV (Supplementary Table S1). The non-specific poly dT spacer sequence at the 5′ end of the primer allowed for the amplification product to warp to an arch shape in solid-phase amplification (Guo et al., 1994). As such, primers were designed that were 10, 20, and 30 bp longer than the conventional primers. Different lengths of MERS primers for detecting MERS and HCoV were immobilized to the microring on the SMR sensor. Subsequently, primers of suitable length for detecting MERS, ZIKV, EBOV, and HCoV were immobilized on the microring resonance sensors. For multiplexing experiments, we used an ultra-small dosage dispensing system with sciFLEXARRAYER SX (SCIENION AG, Monmouth Junction, NJ, USA) to avoid cross-contamination. Subsequently, droplets of other target specific primers solutions were dispensed to the microring at desired locations. Because a smaller amount of primer volume was used than in the previous method, a higher concentration of primer solution was used. Finally, the resonance wavelength shift by products of arch-shaped amplification was measured on the microring.

2.3. End-point and real-time RT-PCR assays

The utility of end-point and real-time reverse transcription PCR were compared to that of the arch-shaped multiple-target assay. We designed RT-PCR primers of standard lengths (approximately 24 bp) based on genome sequence information for MERS, ZIKV, EBOV, and HCoV (Table S1). End-point RT-PCR consist of an initial reverse transcription step at 50 °C for 30 min, followed by at 95 °C for 15 min and 45 cycles at 95 °C for 30 s, 60 °C for 30 s, and 72 °C for 30 s and final elongation step 72 °C for 10 min. The reaction mixtures containing 25 μL of end-point RT-PCR reagent mixtures, 5x one-step RT-PCR buffer (Qiagen One-step RT-PCR kit), 0.25 mM deoxynucleotide triphosphate, 25 pmol of each primer, 1 μL of one-step RT-PCR Enzyme Mix (Qiagen), and 5 μL of RNA template. Gel electrophoresis was used to separate RT-PCR products on a 2% agarose gel containing ethidium bromide (EtBr). The gel was visualized using a GenoSens 1500 gel documentation system (Clinx Science Instruments, Shanghai, China). Real-time RT-PCR consisted of an initial reverse transcription step at 50 °C for 20 min, followed by at 95 °C for 15 min and 45 cycles at 95 °C for 15 s, 60 °C for 20 s, and 72 °C for 20 s, followed by a cooling step at 40 °C for 30 s. The real-time RT-PCR assay was conducted using the manufacturer's protocol (AriaMx, Agilent Technologies, Santa Clara, CA, USA). Additionally, reaction mixtures containing 20 μL of real-time RT-PCR reagent mixtures, 2x brilliant SYBR green RT-qPCR master mix, 25 pmol of each primer, and 5 μL of RNA template were prepared. The amplified products were detected by SYBR Green signals using an AriaMx Real-Time PCR System (AriaMx, Agilent Technologies).

2.4. T7 in vitro transcribed RNA preparation

We generate the T7 *in vitro* transcribed RNAs of MERS, ZIKV, EBOV, and HCoV to assess the detection ability of the Arch-shaped multiple-target assay using the MEGAscript T7 kit (Ambion, Thermo Fisher Scientific, Waltham, MA, USA). For ZIKV, we used the QIAamp viral RNA mini kit (Qiagen, Hilden, Germany) to extract RNA from the medium of the NATtrol Zika Virus, External Run Control containing strain of MR766 (Zeptometrix Corporation, Franklin, MA, USA), which was formulated with purified, intact virus particles chemically modified to render them non-infectious and refrigerator-stable. For EBOV, we used an EBOV Positive Control from the Ebola Virus (EBOV) Real-Time RT-PCR kit containing EBOV NP gene RNA (Liferiver Bio-Tech Corp., San Diego, CA, USA). The amplicons of MERS, ZIKV, EBOV, and HCoV generated in the end-point RT-PCR assay were used to create the T7 *in vitro* transcribed RNA. Synthetic RNA transcripts were purified with a MEGAclear Kit (Ambion, Thermo Fisher Scientific) and quantified using a Nanodrop spectrophotometer (Thermo Fisher Scientific). The purified T7 RNA of MERS, ZIKV, EBOV, and HCoV were stored at −80 °C until use.

2.5. Clinical specimen

To determine the utility of the arch-shaped multiple-target sensor, we used the QIAamp viral RNA mini kit (Qiagen) to extract RNA from 20 nasopharyngeal samples of MERS and HCoV patients. The nasopharyngeal samples were collected from patients at the Asan Medical Center. The Institutional Review Board of Asan Medical Center approved the study protocol, and informed consent was obtained from all participants. We used samples at a starting volume of 200 µL each which were eluted to approximately 60 µL using viral elution buffer. The extracted RNA was screened using the real-time RT-PCR assay for confirmation and stored at −80 °C until further use.

3. Results and discussion

3.1. Design of arch-shaped multiple-target sensing platform

Fig. 1 shows the design of the arch-shaped multiple-target sensing platform for rapid diagnosis of emerging infectious pathogens, such as MERS-CoV, HCoV, ZIKV, and EBOV, using a SMR sensor. We established a series of primers for target amplification and simultaneous detection of specific multiple-targets rather than asymmetric amplification on a SMR sensor lacking multiple target detection (Kim et al., 2018; Koo et al., 2017). For multiple-target sensing, the SMR surface was first amine-modified with APTES and linked to the NH_2-modified 5′-end of both primers. Second, both primers (forward and reverse) of a target were immobilized on the SMR sensor surface. Immobilization of both primers reduces non-specific target binding and false-positives due to primer-dimerization, which leads to the production of non-specific amplicons in the solution. To form an arch-shaped template on the surface, we used longer primers containing non-specific poly dT spacers (Shin et al., 2014). The pair of primers for a single target was immobilized on an individual sensor using a spotting system

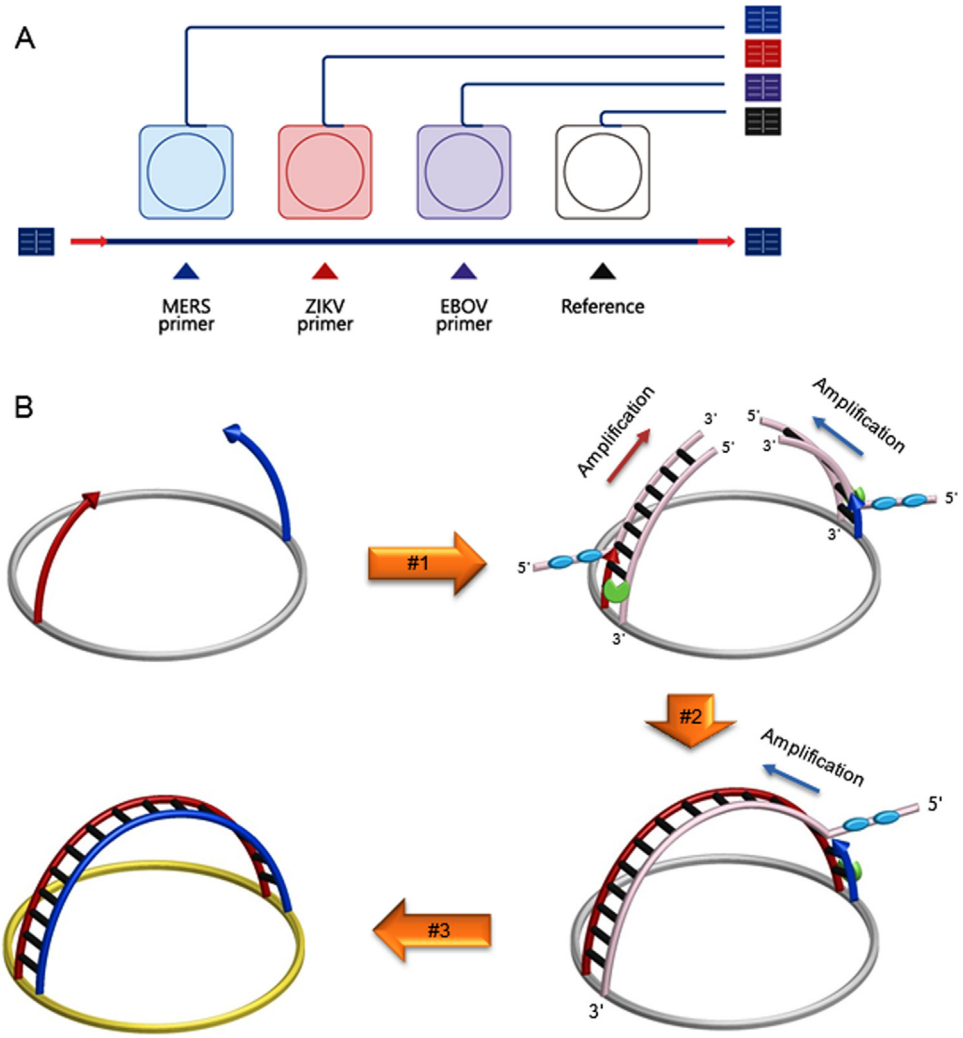

Fig. 1. Scheme of arch-shaped multiple-target sensing platform for diagnosis and identification of emerging infectious pathogens. (A) Array of silicon microring resonator (SMR) sensors for multiple-target detection. Each microring was modified with specific primers (forward and reverse) of MERS-CoV (blue), ZIKV (red), and EBOV (purple) recognizable target sequences. (B) Scheme representation of the principle of arch-shaped amplification and detection assay. First, SMR sensors with specific primers immobilized to detect target RNA were prepared. Next, a mixture containing recombinase polymerase amplification-reverse transcription (RPA-RT) reagent and target extracted RNA was added to the platform (#1). During the reaction, RNA was synthesized by the RPA-RT enzyme mixture in an isothermal state (43 °C) as cDNA and either recombinase/forward (red arrow) primer or recombinase/reverse (blue arrow) primer complexes bound to double-stranded target cDNA and facilitated strand exchange at a constant temperature. After the displaced strand formed a D-loop by gp32 (sky blue), the immobilized primers were extended by polymerase (green) on the sensor surface (#2). The extended primers formed an arch-shaped amplification complex in the same microring and continued amplification (#3). Target detection was monitored in real-time by measuring the resonant wavelength shift by arch-shaped amplified products on the solid surface.

(Supplementary Fig. S1). Third, either RPA or RPA-RT was added for isothermal nucleic acid amplification. During the amplification reaction, both primers were covalently bound to the SMR sensor and target templates were hybridized to both primers. To produce a copy of the hybridized template, RPA enzyme (including Taq polymerase) was activated to amplify the target template on the sensor surface. The attached forward primer bound the template, which could also bind to the attached reverse primer and form additional arch-shaped copies near the initial copies. Finally, we used an SMR sensor, which is a rapid and highly sensitive system for evaluation in a real-time and label-free manner, for the signal readout from multiple sensors. We monitored the resonance wavelength shift changes for up to 30 min. The resonance wavelength shift was obtained by individual sensors using the immobilized specific primers (Fig. 1).

3.2. Optimization of arch-shaped multiple-target sensing platform

We first determined the optimized protocol for arch-shaped multiple-target sensing. Asymmetric amplification (one primer immobilized on a solid surface) generated one of the strands from the target template, and thus the detection sensitivity was less than that of symmetric amplification (Fedurco et al., 2006). Therefore, to overcome the limitations of solid surface amplification methods, the size and concentration of the attached primers should exceed the critical value for efficient amplification on the solid surface. To optimize the primer protocol for multiple-targets, T7 RNA transcripts from a MERS-CoV sample were prepared for the model pathogen. We examined different primer lengths, including a nonspecific oligo-dT sequence, to determine the optimal primer length. The resonance wavelength of 54-bp primers was found to have shifted significantly compared to other primer sizes (Fig. 2 A). Moreover, we determined the concentration of the attached primers (5 μM) (Fig. 2B). A primer concentration of 1 pM resulted in asymmetric amplification, indicating that this concentration was not suitable for the arch-shaped multiple-target sensing platform. Even high concentrations (10 μM) of attached primers could not discriminate between target and non-target templates (Fig. 2B). Therefore, the size and concentration of the attached primers were determined to establish arch-shaped surface amplification on the sensing surface.

3.3. Detection sensitivity and specificity of the arch-shaped multiple-target sensing platform

We next determined the detection sensitivity of the arch-shaped multiple-target sensing platform using MERS-CoV, HCoV, ZIKV, and EBOV as emerging infectious pathogens. T7 RNA transcripts of these pathogens, RNA of MERS-CoV or HCoV from clinical samples, or RNA of ZIKV and EBOV from commercialized kits (positive controls at 10^5 copies/reaction, Fig. 2C) were prepared at varying concentrations of 10–10^5 copies/reaction (Fig. 2C-E). Using the platform, the target RNA (at 10^5 copies/reaction) from the pathogens was clearly identified compared to non-targets within 30 min. The resonance wavelengths were shifted up to 681.48 ± 30.43, 500.75 ± 14.35, 660.55 ± 21.22, and 480.45 ± 28.55 pm for MERS-CoV, HCoV, ZIKV, and EBOV, respectively (Fig. 2D). Interestingly, the resonance wavelength results clearly revealed the target RNA in 5–10 min. Furthermore, we detected as few as 10–100 copies of RNA when serial dilutions of pathogen RNA were used with the platform (Fig. 2E). The wavelength change results showed good linearity with different concentrations (R^2 = 0.9863, 0.9943, 0.9992, and 0.9971 for MERS-CoV, HCoV, ZIKV, and EBOV, respectively) in 30 min. We compared the RPA and SMR assay using this multiple-target sensor assay (Supplementary Fig. S2). After confirming the detection of the amplified EBOV target in the RPA assay, the target band was clearly distinguished down to 5 × 10^3 copies/reaction (Supplementary Fig. S2A). Additionally, after confirming the detection of the amplified MERS target in the SMR assay, the target was clearly distinguished down to 2.5 × 10^2 copies/reaction (Supplementary Fig. S2B). Notably, the sensitivity of the multiple-target sensing platform was 10–100-fold higher than that (10^3 copies/reaction) of the quantitative real-time reverse transcription PCR, RPA, and SMR assays (Table 1, Supplementary Fig. S2 and Fig. S3).

Subsequently, we used the multiple-target sensing platform to identify different targets. A series of target primers from three pathogens, specifically MERS-CoV, ZIKV, and EBOV, was immobilized to the individual sensor with the spotting machine, which can immobilize the primer in a specific area (Fig. 3A). Using the specific attached primers for MERS-CoV, the amplified MERS-CoV RNA was detected with low background signals from other pathogens (Fig. 3B). Similarly, primers for other pathogens showed high specificity with low non-target binding (Fig. 3B). Additionally, when mixed virus (MERS and HCoV) samples were used, the resonance wavelength shift of the MERS-specific primer immobilized on the platform was 560.71 ± 28.51 pm when only MERS (2.5 × 10^4 copies/reaction) virus was present and was 572.98 ± 11.05 pm when both MERS (2.5 × 10^4 copies/reaction) and HCoV (1.5 × 10^4 copies/reaction) viruses were present. The resonance wavelength analysis clearly detected the target RNA in the mixed virus samples, which showed similar results to the use of the single virus sample (Supplementary Fig. S4). Indeed, a rapid, high-sensitivity, and high-specificity platform for multiple-target detection is needed for emerging pathogen diagnosis. The arch-shaped multiple-target sensing platform enables rapid and accurate pathogen genotyping.

3.4. Clinical testing of arch-shaped multiple-target sensing platform in clinical specimens

We evaluated the clinical utility of the arch-shaped multiple-target sensing platform using clinical specimens (Supplementary Fig. S5). Particularly, methods for differentiating emerging infectious pathogens from similar pathogens are needed. In 2015, there was a MERS-CoV outbreak in Korea. During this outbreak, diagnostic platforms were urgently needed to differentiate between MERS-CoV and HCoV to ensure specific treatment. To optimize the multiple-target sensing for MERS-CoV prior to use in clinical samples, T7 of *in vitro*-transcribed MERS-CoV and HCoV-OC43 RNA was prepared. Two sensing microrings for the MERS-CoV and HCoV primers were in the same waveguide. Subsequently, the RNA template of either MERS-CoV or HCoV was added onto the platform (Fig. 4A-B). To eliminate the background signal from non-target binding, we used the following equation:

$$\Delta\Delta RWS = \frac{\text{Individual resonant wavelength shift value of target}}{\text{Highest resonant wavelength shift value of non target}}$$

Using the MERS-CoV primers with the equation, amplified RNA from MERS-CoV was detected with no signal from HCoV from 5 to 30 min. Additionally, using the HCoV primers, amplified RNA from HCoV was detected, while MERS-CoV was not (Fig. 4A–B). Further, the relative resonance wavelength shifts clearly distinguished positive and negative results when detecting multiple targets.

Finally, we analyzed RNAs from 20 clinical nasopharyngeal samples, including those of 11 MERS-CoV infected patients collected from July 2015 in South Korea and 9 HCoV-OC43 infected patients (Fig. 4C–D). Patient samples were analyzed by quantitative real-time reverse transcription PCR (procedural time, 2–3 h) and the arch-shaped multiple-target sensing platform (procedural time, 20 min). For clinical testing (sensitivity and specificity) of the multiple-target sensing platform, we added RNA from MERS-CoV patients into the platform, which included immobilized primers with either MERS-CoV or HCoV on an individual sensing ring. The wavelength shifted to higher than 220.83 pm in the MERS-CoV sensing ring; however, the wavelength shifted to lower than 146.24 pm in the HCoV-OC43 sensing ring. In contrast, when the RNA of HCoV-OC43 patients was added, the wavelength shifted to higher than 220.29 pm in the HCoV-OC43 sensing ring and shifted to lower than 143.55 pm in the MERS-CoV sensing ring. These results confirm that the arch-shaped multiple-target sensing platform can accurately identify MERS-CoV or HCoV in clinical samples

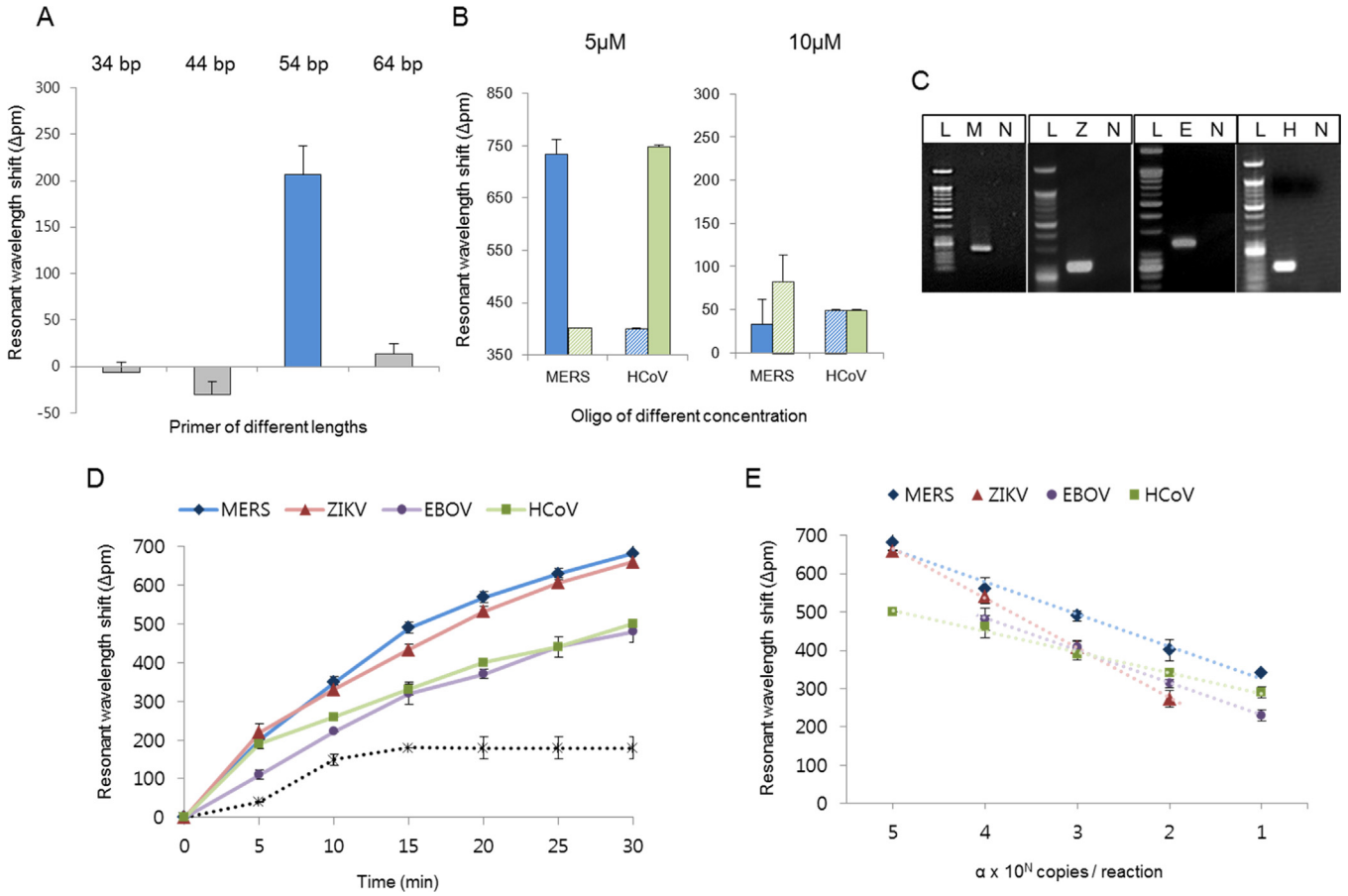

Fig. 2. Detection sensitivity of the arch-shaped multiple-target sensing. (A) Primer length testing for formation of the arch-shape. Monitoring of resonance wavelength shift by different oligonucleotide lengths of the MERS-specific primer immobilized on the sensor. (B) Primer concentration testing. Monitoring of resonance wavelength shift by different concentrations (5 and 10 μM) of the MERS (blue) and HCoV (green)-specific primer immobilized on the sensor for multiple-target detection. (C) Gel electrophoresis data for end-point RT-PCR products from MERS, ZIKV, EBOV, and HCoV (L: 50-bp DNA marker, M: MERS RNA template, Z: ZIKV RNA template, E: EBOV RNA template, H: HCoV RNA template, N: Negative control). (D) Resonance wavelength shift using the arch-shaped multiple-target sensing platform showing results of amplification and detection of MERS (blue diamond), ZIKV (red triangle), EBOV (purple circle), HCoV (green square), and negative control (non-target RNA, black asterisk) in a label-free and real-time manner. (E) Linear relationship between resonance wavelength shift by arch-shaped sensing platform and the concentration of targets in 30 min. Error bars indicate standard deviation of the mean based on at least 3 independent experiments.

Table 1
Results of arch shaped multiple-target sensing and concentration conversion of clinical specimens.

Clinical specimens		Arch shaped Wavelength shift (Δpm)	Concentration conversion (Copies/reaction)
MERS CoV	M1	290.2850	18.54
	M2	260.0750	8.78
	M3	349.4950	80.15
	M4	250.3550	6.91
	M5	269.8850	11.20
	M6	220.8333	3.33
	M7	230.6250	4.24
	M8	270.9750	11.50
	M9	370.4750	134.64
	M10	338.2850	60.75
	M11	299.9700	23.56
HCoV OC43	H1	490.3800	6.67×10^4
	H2	250.3900	5.79
	H3	500.1245	9.75×10^4
	H4	410.8400	3.01×10^3
	H5	220.2900	1.79
	H6	627.3533	1.39×10^7
	H7	240.1750	3.89
	H8	359.6900	4.10×10^2
	H9	330.2550	1.30×10^2

(Fig. 4, Supplementary Fig. S5, and Table 2).

4. Conclusions

Since the advent of solid-phase amplification technologies, asymmetric and bridge-based amplification approaches have been established. However, the amplification efficiency of these methods is too low for clinical use (Adessi et al., 2000; Fedurco et al., 2006; Shendure and Ji, 2008). In this study, we developed a method for enhancing the sensitivity of solid-phase amplification approaches by using an optimal length (about 50 bp) and concentration (5 μM) of oligonucleotide primers within the SMR sensor. Using this platform, inhibition due to primer-dimerization can be prevented during multiple-target detection. Further, we performed diagnostic and identification testing on the platform using several emerging infectious pathogens, such as MERS-CoV, HCoV, ZIKV, and EBOV. We compared the arch-shaped multiple-target sensing platform results to those obtained by PCR (Table 2). Based on the results, the platform showed high accuracy for detecting all pathogen types identified by PCR. Additionally, the detection limit of the platform was superior to that of the conventional method. Therefore, this method can be used for early diagnosis and identification of pathogens in low-level pathogen samples. This platform has advantages over the isothermal, PCR, and bio-optical sensing systems, particularly in terms of time (< 20 min) and label-free detection.

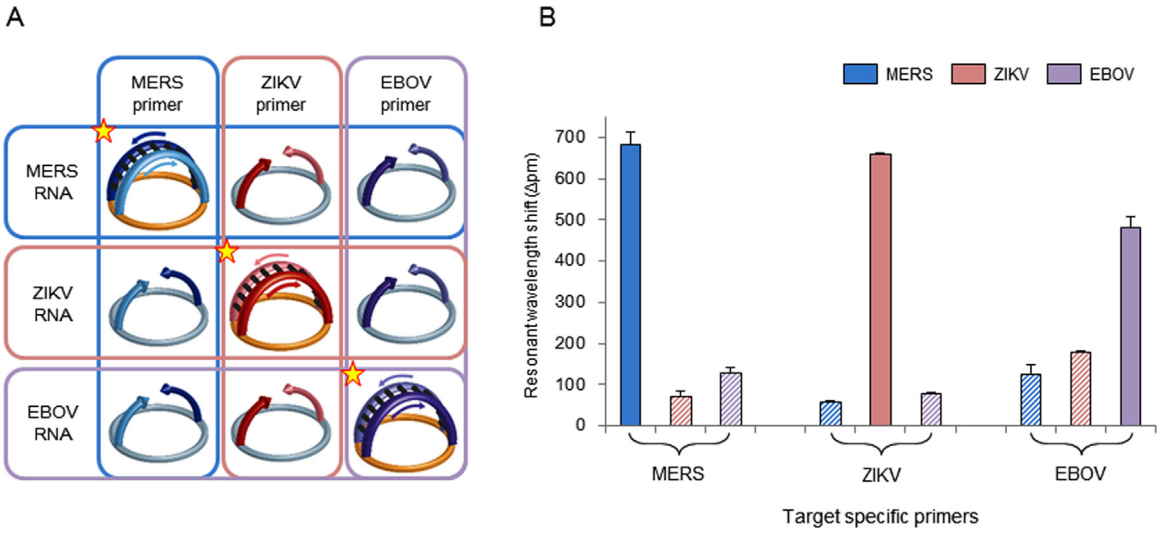

Fig. 3. Cross-reactivity testing of the arch-shaped multiple-target sensing. (A) Scheme of the arch-shaped amplification and detection using different target RNAs and different target specific primers of MERS, ZIKV, and EBOV on the individual sensing platform. (B) Resonance wavelength shift by target RNA and target specific primers for MERS, ZIKV, and EBOV detection on the sensor. Error bars indicate standard deviation of the mean based on at least 3 independent experiments.

Furthermore, the clinical utility of the platform for identifying multiple pathogens in clinical samples is useful for overcoming the limitations of conventional approaches. Further in-depth studies to maximize the clinical ability of the platform in larger prospective clinical trials are needed. Therefore, the arch-shaped multiple-target sensing platform can be used for rapid diagnosis and identification of pathogens in various clinical applications.

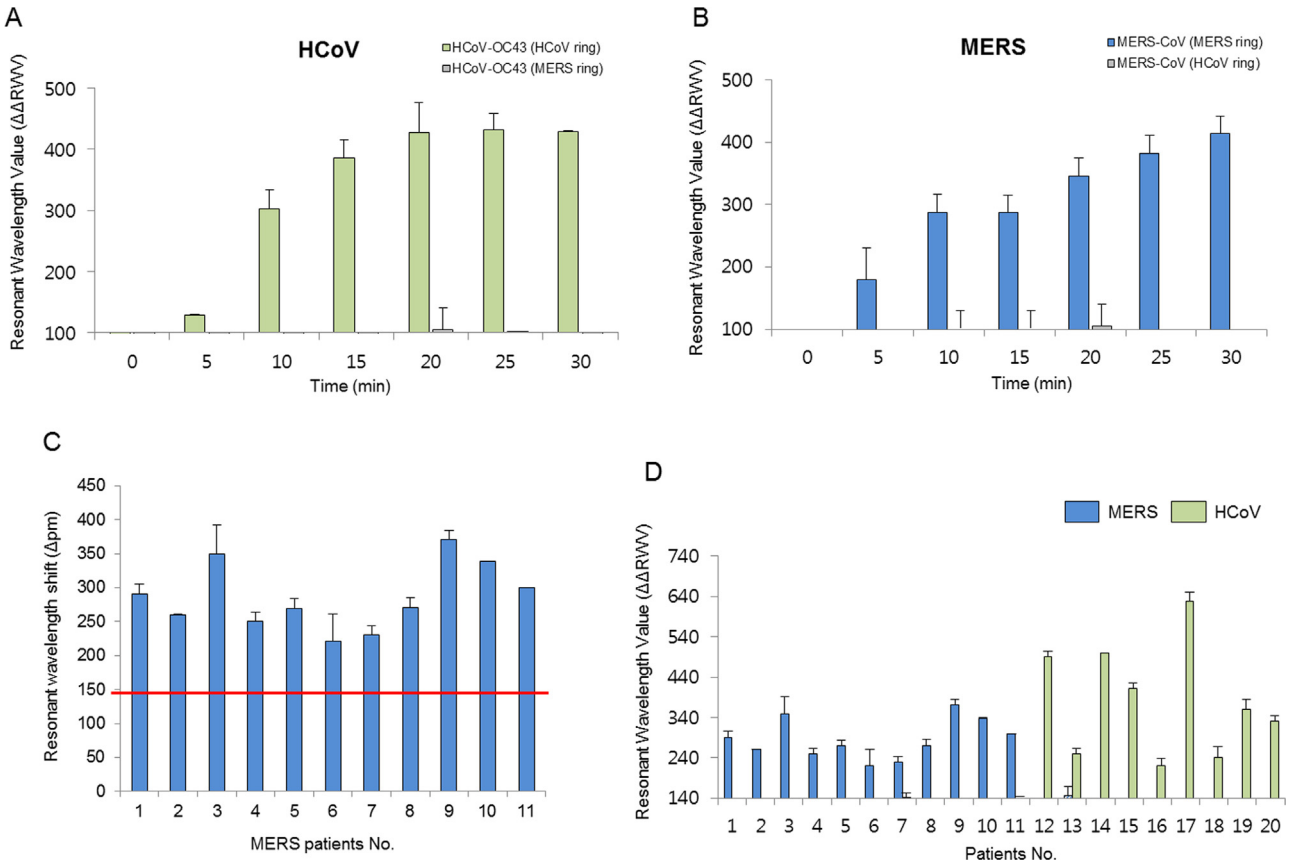

Fig. 4. Clinical utility of the arch-shaped multiple-target sensing platform in clinical specimens. (A–B) Multiple-target testing for detection of MERS-CoV and HCoV on different target specific primers immobilized on individual sensor microrings on an array. (A) Resonance wavelength value of HCoV into the platform. (B) Resonance wavelength value of MERS-CoV into the platform. (C) Analysis of 11 RNAs from clinical samples of MERS patients in 30 min. The red line represents the cut-off (criterion) for reporting a sample as virus (positive/negative). (D) Clinical diagnostic testing using 20 clinical samples, including 11 MERS patients (No. 1–11) and 9 HCoV patients (No. 12–20). Error bars indicate standard deviation of the mean based on at least 3 independent experiments.

Table 2
Comparison of the arch-shaped multiple-target sensor, previous single-target sensor and real-time RT-PCR assay.

Contents		Arch-shaped Multiple targets	SMR Single target	Conventional Real-time PCR
Primer state	Forward	Immobilized	Immobilized	Soluble
	Reverse	Immobilized	Soluble	Soluble
Primer-Dimerization		X	△	○
Amplification method		Isothermal (38–43 °C)	Isothermal (38–43 °C)	Thermocycler (95 °C → 60 °C → 72 °C)
Reaction time		20 min	20 min	2 h
Detection		Label-free Real-time	Label-free Real-time	Labeled (Fluorescence) Real-time
Detection Limit (copies/reaction)	MERS	10^1	10^2	10^3
	ZIKV	10^2	NT	10^3
	EBOV	10^1	NT	10^3
	HCoV	10^1	10^2	10^3
Principle of Detection		Arch-shaped amplification (Label-free)	NT	Probe-based detection (Labeled)

NT: Not tested.

Acknowledgements

This study was supported by a grant from the Korea Health Technology R & D Project through the Korea Health Industry Development Institute (KHIDI), funded by the Ministry of Health & Welfare, Republic of Korea [HI15C-2774–020015].

Appendix A. Supporting information

Supplementary data associated with this article can be found in the online version at doi:10.1016/j.bios.2018.08.007.

References

Adessi, C., Matton, G., Ayala, G., Turcatti, G., Mermod, J.J., Mayer, P., Kawashima, E., 2000. Solid phase DNA amplification: characterisation of primer attachment and amplification mechanisms. Nucleic Acids Res. 28 (20) (e87-e87).

Allegranzi, B., Nejad, S.B., Combescure, C., Graafmans, W., Attar, H., Donaldson, L., Pittet, D., 2011. Burden of endemic health-care-associated infection in developing countries: systematic review and meta-analysis. Lancet 377 (9761), 228–241.

Barken, K.B., Haagensen, J.A., Tolker-Nielsen, T., 2007. Advances in nucleic acid-based diagnostics of bacterial infections. Clin. Chim. Acta 384 (1–2), 1–11.

Biava, M., Colavita, F., Marzorati, A., Russo, D., Pirola, D., Cocci, A., Petrocelli, A., Delli Guanti, M., Cataldi, G., Kamarad, T.A., Kamarad, A.S., Konnehd, K., Cannas, A., Coen, S., Quartu, S., Meschi, S., Valli, M.B., Mazzarelli, A., Venditti, C., Grassi, G., Rozera, G., Castilletti, C., Mirazimi, A., Capobianchi, M.R., Ippolito, G., Miccio, R., Di Caro, A., 2018. Evaluation of a rapid and sensitive RT-qPCR assay for the detection of Ebola Virus. J. Virol. Methods 252, 70–74.

Brinkmann, A., Ergünay, K., Radonić, A., Tufan, Z.K., Domingo, C., Nitsche, A., 2017. Development and preliminary evaluation of a multiplexed amplification and next generation sequencing method for viral hemorrhagic fever diagnostics. PLoS Negl. Trop. Dis. 11 (11), e0006075.

Chung, H.J., Castro, C.M., Im, H., Lee, H., Weissleder, R., 2013. A magneto-DNA nanoparticle system for rapid detection and phenotyping of bacteria. Nat. Nanotechnol. 8 (5), 369.

Fedurco, M., Romieu, A., Williams, S., Lawrence, I., Turcatti, G., 2006. BTA, a novel reagent for DNA attachment on glass and efficient generation of solid-phase amplified DNA colonies. Nucleic Acids Res. 34 (3) (e22-e22).

Guo, Z., Guilfoyle, R.A., Thiel, A.J., Wang, R., Smith, L.M., 1994. Direct fluorescence analysis of genetic polymorphisms by hybridization with oligonucleotide arrays on glass supports. Nucleic Acids Res. 22 (24), 5456–5465.

Huang, F.C., Liao, C.S., Lee, G.B., 2006. An integrated microfluidic chip for DNA/RNA amplification, electrophoresis separation and on-line optical detection. Electrophoresis 27 (16), 3297–3305.

Kim, J.Y., Koo, B., Jin, C.E., Kim, M.C., Chong, Y.P., Lee, S.O., Choi, S.H., Kim, Y.S., Woo, J.H., Shin, Y., Kim, S.H., 2018. Rapid diagnosis of tick-borne illnesses by use of one-step isothermal nucleic acid amplification and bio-optical sensor detection. Clin. Chem. 64 (3), 556–565.

Koo, B., Jin, C.E., Lee, T.Y., Lee, J.H., Park, M.K., Sung, H., Park, S.Y., Lee, H.J., Kim, S.M., Kim, J.Y., Kim, S.H., Shin, Y., 2017. An isothermal, label-free, and rapid one-step RNA amplification/detection assay for diagnosis of respiratory viral infections. Biosens. Bioelectron. 90, 187–194.

MERS-CoV | Prevention and Treatment of MERS | Coronavirus | CDC. 〈www.cdc.gov〉. 13 July 2016.

Mori, Y., Notomi, T., 2009. Loop-mediated isothermal amplification (LAMP): a rapid, accurate, and cost-effective diagnostic method for infectious diseases. J. Infect. Chemother. 15 (2), 62–69.

Munoz-Jordan, J.L., 2017. Diagnosis of Zika virus infections: challenges and opportunities. J. Infect. Dis. 216 (suppl_10), S951–S956.

Piepenburg, O., Williams, C.H., Stemple, D.L., Armes, N.A., 2006. DNA detection using recombination proteins. PLoS Biol. 4 (7), e204.

Rao, S., Nyquist, A.C., 2014. Respiratory viruses and their impact in healthcare. Curr. Opin. Infect. Dis. 27 (4), 342–347.

Sands, P., Mundaca-Shah, C., Dzau, V.J., 2016. The neglected dimension of global security—a framework for countering infectious-disease crises. N. Engl. J. Med. 374 (13), 1281–1287.

Shendure, J., Ji, H., 2008. Next-generation DNA sequencing. Nat. Biotechnol. 26 (10), 1135.

Shin, Y., Kim, J., Lee, T.Y., 2014. A solid phase-bridge based DNA amplification technique with fluorescence signal enhancement for detection of cancer biomarkers. Sens. Actuators B: Chem. 199, 220–225.

World Health Organization, 2015a. Middle East Respiratory Syndrome Coronavirus (MERS-CoV): Summary of Current Situation, Literature Update And Risk Assessment. WHO, Geneva, Switzerland.

World Health Organization, 2015b. Laboratory Testing for Middle East Respiratory Syndrome Coronavirus (MERS-CoV): Interim Guidance. World Health Organization, Geneva.

World Health Organization, 2016a. Middle East Respiratory Syndrome Coronavirus (MERS-CoV). WHO, Geneva, Switzerland.

Yang, S., Rothman, R.E., 2004. PCR-based diagnostics for infectious diseases: uses, limitations, and future applications in acute-care settings. Lancet Infect. Dis. 4 (6), 337–348.

Zaki, A.M., Van Boheemen, S., Bestebroer, T.M., Osterhaus, A.D., Fouchier, R.A., 2012. Isolation of a novel coronavirus from a man with pneumonia in Saudi Arabia. N. Engl. J. Med. 367 (19), 1814–1820.

Zumla, A., Hui, D.S., Perlman, S., 2015. Middle East respiratory syndrome. Lancet 386 (9997), 995–1007.